The Impact Toughness of C–Mn Steel Arc–Welds – A Bayesian Neural Network Analysis

H. K. D. H. Bhadeshia*, D. J. C. MacKay* and L.–E. Svensson†

*Mathematics and Physical Sciences Group
Darwin College, Silver Street, Cambridge CB3 9EU, U. K

†Central Research Laboratories, ESAB AB
Gothenburg, Sweden

ABSTRACT

Charpy impact toughness data for manual metal arc and submerged arc weld metal samples have been analysed using a neural network technique within a Bayesian framework. In this, the toughness can be represented as a general empirical function of variables that are commonly acknowledged to be important in influencing the properties of steel welds. The method has limitations due to its empirical character, but it is demonstrated here that it can be used in such a way that the predicted trends make metallurgical sense. The method has been used to examine the relative importance of the numerous variables thought to control the toughness of welds.

INTRODUCTION

Fusion welding is of the greatest importance in the fabrication of engineering structures. One of the most important requirements for such structures, including all the welded joints, is that they should be able to resist brittle fracture. The weld deposits therefore have to be "tough" with a great deal of energy being absorbed by the metal during the process of fracture.

A test used to characterise toughness is the Charpy test, in which a square sectioned, notched bar is fractured under specified conditions [1]. The energy absorbed during fracture is taken as a measure of toughness. The Charpy test is empirical in that the data cannot be used directly in engineering design. It is nevertheless a useful quality control test which is specified widely in international standards, and in the ranking of samples in research and development experiments.

The toughness of a steel depends on many variables, and that of a weld on many more because of the complexity of the welding process. It is not yet possible to predict the Charpy toughness of a weld with any reliability. The usual approach is to correlate the results against chosen variables using linear regression analysis [*e.g.* 2]. These methods are known to be severely limited in their application.

Therefore, the most important mechanical property for welds has not been rationalised quantitatively as a function of the complex array of variables associated with welding. However, it is known from experience, and from the concepts of fracture mechanics, that certain variables are more important than others in their effect on toughness. The purpose of the work presented here was to see whether an artificial neural network [3] can be trained to predict weld toughness as a nonlinear function of these variables, and to see whether the patterns that emerge from the work emulate metallurgical experience.

In normal regression methods the analysis begins with the prior choice of a relationship (usually linear) between the output and input variables. A neural network is capable of realising a greater variety of nonlinear relationships of considerable complexity. Data are presented to the network in the form of input and output parameters, and the optimum non–linear relationship is found by minimising a penalized likelihood. The network in effect tries out many kinds of relationships in its search for an optimum fit. As in regression analysis, the results then consist of a specification of the function, which in combination with a series of coefficients (called weights), relates the inputs to the outputs. The search for the optimum representation can be computer intensive, but once the process is completed (*i.e.* the network trained) the estimation of the outputs is very rapid. In spite of its apparent sophistication, the method is as blind as regression analysis, and neural nets can be susceptible to overfitting.

However, much of this danger can in principle be minimised or eliminated by combining the neural network approach with sound statistical and metallurgical theory. MacKay [4–7] has developed a Bayesian framework for neural networks. This framework allows one to assess quantitatively the relative probabilities of models of different complexity, and to put quantitative error bars on the predictions of the models. We have applied this work to the complex problem of predicting weld metal toughness.

VARIABLES

It is possible to choose a set of variables which should, using experience of welding metallurgy, have an influence of the Charpy toughness. These variables are listed in Table 1, and described below.

In general, the toughness decreases as the strength increases. This is because plastic deformation, which is the major energy absorbtion mechanism during fracture, becomes more difficult as the strength increases. Hence, the yield strength is included as a variable. The nature of the welding process itself may have a significant effect on toughness. For example, the submerged arc welding process is quite different from the manual metal arc welding process,

Variable	Range	Mean	Standard Deviation
Process	Submerged Arc		
	Manual Metal Arc		
Yield Strength MPa	347–645	471	12.7
Carbon wt.%	0.029–0.13	0.08	0.004
Silicon wt.%	0.28–1.14	0.49	0.05
Manganese wt.%	0.77–2.50	1.32	0.07
Phosphorus wt.%	0.008–0.028	0.015	0.001
Sulphur wt.%	0.002–0.017	0.010	0.0005
Aluminium wt.%	0.001–0.04	0.014	0.002
Nitrogen p.p.m.w.	26–119	67	4
Oxygen p.p.m.w.	234–821	412	30
Primary Microstructure %	0–91	34	4
Secondary Microstructure %	9–100	66	2
Allotriomorphic Ferrite %	16–62	31	2
Acicular Ferrite %	11–81	55	2
Widmanstätten Ferrite %	0–35	14	2
Temperature K	213–293	259	25
Charpy Toughness J	4–215		

Table 1: The variables. The abbreviation p.p.m.w. stands for parts per million by weight.

leading to the development of different microstructures and variations in impurity content. However, heat input *per se* is not included since its effect is via the microstructure [8–12], which is included in detail in the analysis.

The major solute additions to steels, *i.e.* C, Mn and Si, have large effects on the transformation behaviour and strength. Impurity elements (P, S, Al, N, O) are included because of their known tendency to embrittle or because of their importance in the formation of non-metallic inclusions in welds.

All fusion welding processes involve the deposition of a small amount of molten steel within a gap between the components to be joined. When the steel solidifies, it welds the components together. The *fusion zone* represents both the deposited metal and the parts of the steel component melted during the process, and is a solidification microstructure, often called the *primary microstructure*. In practice, the gap between the components to be joined has to be filled by a sequence of several weld deposits. These multirun welds have a complicated microstructure. The deposition of each successive layer heat–treats the underlying microstructure. Some of the regions of original primary microstructure are reheated to temperatures high enough to cause the reformation of austenite, which during the cooling part of the thermal cycle transforms into a different microstructure. Other regions may simply be tempered by the deposition of subsequent runs. The microstructure of the reheated regions is called the *reheated* or *secondary* microstructure. The fractions of the primary and secondary microstructures are included as input variables (Table 1).

In addition, the details of the primary microstructure are also included in the list of input variables, since the phases involved (allotriomorphic, Widmanstätten and acicular ferrite) are known to have a major influence on the weld properties.

Iron undergoes a ductile–brittle transition as a function of temperature [1]. The flow stress of iron is sensitive to temperature, the strength increasing as the temperature decreases. At some critical temperature, it becomes easier to cleave iron without expending much energy. Below this critical temperature, the iron behaves in a very brittle manner. Hence, the test temperature is included as an important variable.

All of these input variables should to varying degrees influence the Charpy toughness, which is the output variable.

EXPERIMENTAL DATA

All of the data used in the analysis are from experiments conducted at the ESAB Central Research Laboratories [13–15]. These data represent a total of 181 different combinations of the variables listed in Table 1, from all–weld metal tests in which the joints were deposited to ISO2560 specification as described elsewhere [11]. In this specification, the joint geometry is such that there is a minimal dilution of the weld metal, so that experiments can be conducted on all–weld samples. Hence, the development of welding electrodes is usually carried out using this joint design. References 13 and 15 contain data on manual metal arc welds where as Ref. 14 deals with submerged arc welds. All of these welds are typically classified as carbon–manganese welds, because they do not contain deliberate additions of elements such as nickel, boron *etc.*

The manual metal arc welds were deposited in the flat position using the stringer bead technique, the parent plate thickness being 20 mm. The welding current and voltage used were 190 A and 23 V respectively, the weld consisting of some 27 runs with 3 runs per layer deposited at a speed of 0.004 $\mathrm{m\,s^{-1}}$. The interpass temperature was typically 250 °C. The electrodes used were 4 mm in diameter.

The submerged arc welds were fabricated to the same geometry, but with a variety of proprietary wires and flux combinations. The wires were of 4 mm diameter (*OK Autrod* 12.10, 12.22 & 12.32) and the fluxes included *OK Flux* 10.61, 10.71 and 10.81. The terms in italics are trade marks of ESAB AB – there is nothing special about these consumables but is worth noting that they are all commonly used in welding mild steels. The significant welding parameters are listed in Table 2; the interpass temperature was about 250 °C in each case.

Current Amps	Voltage	No. of Beads	Welding Speed $\mathrm{m\,s^{-1}}$
450	30	14–16	0.007
550	30	12	0.007
650	30	10	0.007

Table 2: Welding parameters for the submerged arc welds.

The tests have been carried out over a number of years with the systematic measurement of all of the important parameters discussed earlier. However, the fraction of primary and secondary microstructure was not measured for the data in [14]. These fractions were therefore calculated as described in [9,16].

The routine method for quantitative metallography has been described previously [11], and the mechanical property measurements were carried out to ISO2560 specification. The Charpy value used in the analysis represented the mean of between three to five tests.

ANALYSIS

The analysis was conducted using variables normalised between +0.5 and -0.5; this normalisation is not essential to the neural net approach but allows a convenient comparison of the influence of individual input variables on an output. The normalisation procedure is expressed quantitatively as follows:

$$x_N = \frac{x - x_{min}}{x_{max} - x_{min}} - 0.5 \tag{1}$$

where x_N is the normalised value of x; x_{min} and x_{max} are respectively the minimum and maximum values of x in the entire dataset (Table 1).

The normalisation is straightforward for all the quantitative variables; however, the welding process was represented by assigning a value of +0.5 to submerged arc welding, and -0.5

to manual metal arc welding.

The network consisted of fourteen input nodes, a number of hidden nodes and an output node representing the toughness (Fig. 1). The network was trained using a randomly chosen 100 of the examples from a total of 181 available, the remaining 81 examples being used as ‘new’ experiments to test the trained network.

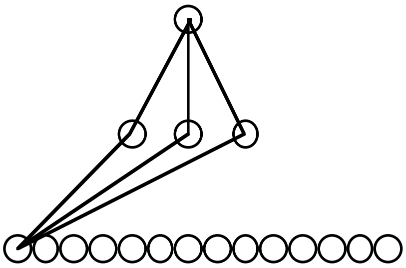

Fig. 1: A typical network used in the analysis. Only the connections originating from one input unit are illustrated, and the two bias units are not illustrated.

Linear functions of the inputs x_j are operated on by a hyperbolic tangent transfer function:

$$h_i = \tanh\left(\sum_j w_{ij}^{(1)} x_j + \theta_i^{(1)}\right) \tag{2}$$

so that each input contributes to every hidden unit. The bias is designated θ_i and is analogous to the constant that appears in linear regression. The strength of the transfer function is in each case determined by the weight w_{ij}. The transfer to the output y is linear:

$$y = \sum_i w_i^{(2)} h_i + \theta^{(2)} \tag{3}$$

This specification of the network structure, together with the set of weights is a complete description of the formula relating to the inputs to the output. The weights are determined by training the network; the details are described elsewhere [4–7]. The training involves a minimisation of the regularised sum of squared errors. The term σ_ν used below is the framework estimate of the noise level of the data.

The complexity of the model is controlled by the number of hidden units (Fig. 2), and the values of the 16 regularisation constants (σ_w), one associated with each input, one for biases and one for all weights connected to the output.

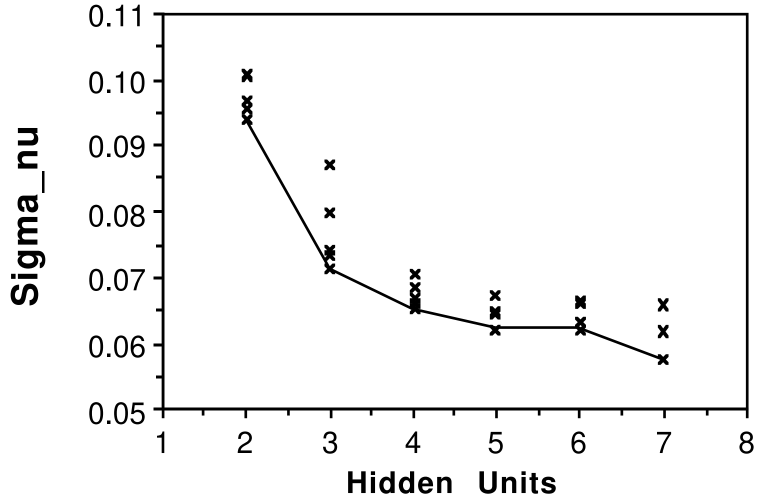

Fig. 2: Variation in σ_ν as a function of the number of hidden units. Several values are presented for each set of hidden units because the training for each network was started with a variety of random seeds.

Fig. 2 shows that the inferred noise level decreases monotonically as the number of hidden units increases. However, the complexity of the model also increases with the number of hidden units. A high degree of complexity may not be justified, and in an extreme case, the model may in a meaningless way attempt to fit the noise in the experimental data. MacKay [4–7] has made a detailed study of this problem and has defined a quantity (the *evidence*) which comments on the probability of a model. In circumstances where two models give similar results over the known dataset, the more probable model would be predicted to be that which is simpler; this simple model would have a higher value of 'evidence'. The evidence framework was used to control the regularisation constants and σ_ν. The number of hidden units was set by examining performance on test data. A combination of Bayesian and pragmatic statistical techniques were therefore used to control the model complexity. Four hidden units were found to give a reasonable level of complexity to represent the variations in toughness as a function of the input variables. Larger numbers of hidden units did not give significantly lower values of σ_ν; indeed, the test set error goes through a minimum at four hidden units (Fig. 3).

The optimum parameters for one trained network are presented in Table 3; this listing would be required in order to reproduce the predictions described, though not the error bars. The levels of agreement for the training and test datasets are illustrated in Fig. 4, which show good prediction in both instances. It should be emphasized that the test data were not included

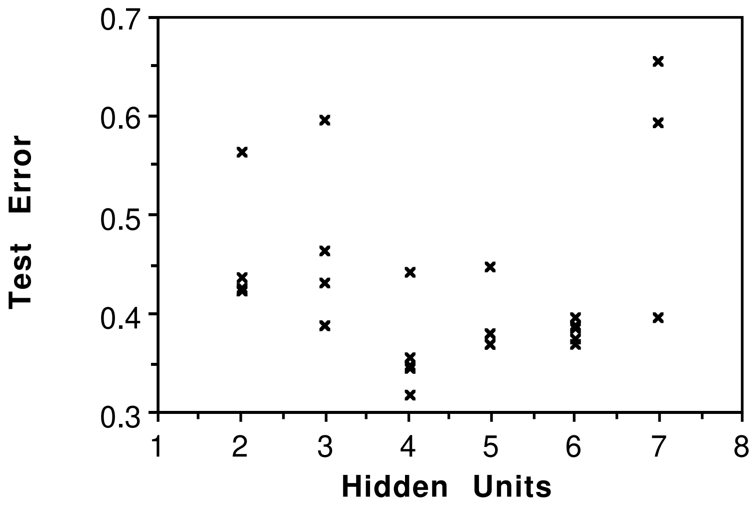

Fig. 3: The test error as a function of the number of hidden units.

in deriving the weights given in Table 3 (except to choose the solution displayed), so that the good fit is established to work well over the range of data included in the analysis.

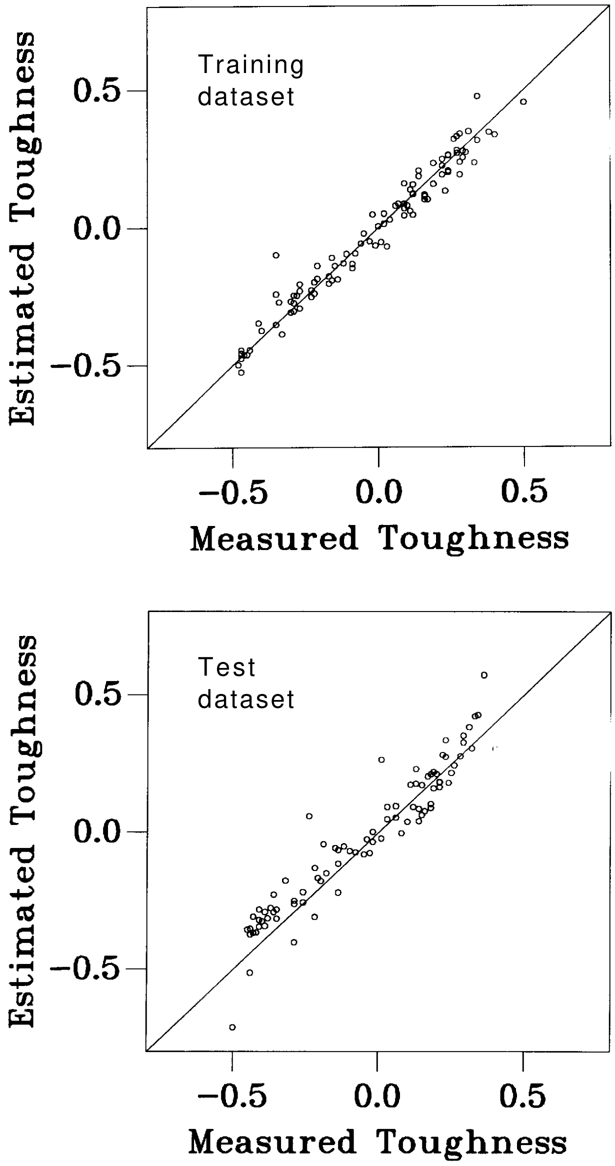

Fig. 4: Plot of the estimated versus measured toughness; (a) training dataset; (b) test dataset.

USE OF THE MODEL

We now examine the metallurgical significance of the results. We attempt predictions out of the range of the experimental data used during training, and examine some aspects which cannot be studied experimentally.

Fig. 5 illustrates the significance (σ_w) of each of the input variables, as perceived by the neural network, in influencing the toughness of the weld. The process clearly has a large intrinsic effect, which complies with experience in that submerged arc welds are in general of a lower quality than manual metal arc welds. Note that this is a process effect which is independent of all the other variables listed. The yield strength has a large effect and that is well established [1]. It is also widely believed, as seen in Fig. 5, that acicular ferrite has a large effect on the toughness. Nitrogen has a large effect, as is well established experimentally [10,17–12]. Oxygen influences welds in both beneficial and harmful ways, *e.g.* by helping the nucleation of acicular ferrite or contributing to fracture by nucleating oxides.

It is surprising at first sight that carbon has such a small effect, but what the results really demonstrate is that the influence of carbon comes in via the strength and microstructure. Phosphorus and sulphur have only a small effect; the toughness measured was in the as–welded condition whereas many of the classical embrittlement effects manifest themselves in the stress–relieved condition. It is also possible that the effects of P and S are higher at strength levels larger than encountered here. All of the welding consumables are commercially used so that they are not expected to be embrittlement prone. Elements such as Mn and Si do not feature greatly presumably because their effect comes in via microstructure. Fig. 5 also shows a relatively small effect of temperature on toughness, but it should be noted that the temperature range considered is only 80 °C (Table 1), and that a part of the effect of temperature is to alter the yield strength, which is identified by the model to be one of the important variables.

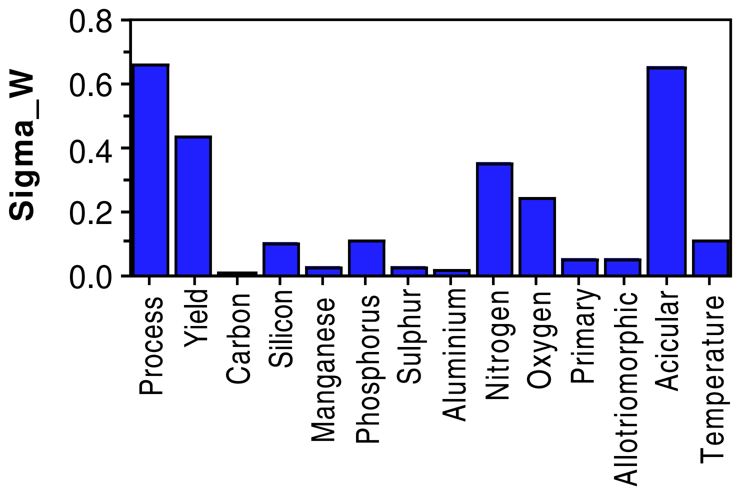

Fig. 5: Bar chart showing a measure of the model–perceived significance of each of the input variables in influencing toughness.

The model can be used to estimate the toughness if all of the inputs listed in Table 1 are available. The amount of work required to accumulate these inputs is not trivial, but the situation can be ameliorated. A physical model [11,12,16] based on phase transformation theory can be used to predict the values of all the inputs from a knowledge of just the chemical composition and a choice of welding conditions. This was done particularly to examine the effects of carbon and manganese on weld toughness, given that a lot of work on these lines has already been reported in the literature.

Fig. 6a shows data generated using the neural network but with all the inputs other than manganese calculated using our weld model [11,12,16]. In all cases, the calculated inputs are for manual metal arc welds with 180 A, 34 V, a welding speed of 0.004 $\mathrm{m\,s^{-1}}$, interpass temperature 200 °C, ISO2569 weld geometry. The manganese variations are for a basic composition

$$\mathrm{Fe - 0.07C - 0.5Si - Mn - 0.005S - 0.0025O - 0.0005N - 0.025Al}$$

. It is interesting that the toughness at relatively high temperatures decreases as the manganese concentration is increased. This upper shelf region involves ductile failure, and an increase in strength leads to a reduction in the ductile fracture energy. The calculated yield strength [10,12,16] increases from 403–539 MPa as the Mn concentration is changed from 0.5-2.0 wt.%. However, the cleavage toughness at low temperatures clearly increases with Mn up to a concentration of 1.5 wt.%. This is because the calculated [10,12,16] acicular ferrite content increases from 35-67% when Mn is changed over the range illustrated. The low temperature toughness for 2 wt.% Mn is nevertheless lower than that for the 1.5 wt.% alloy presumably because the increased acicular ferrite content is not sufficient to compensate for the increased strength. Indeed, an optimum manganese concentration of about 1.5 wt.% has been reported to achieve the best toughness in manual metal arc welds of the type discussed here [22,23].

Fig. 6b shows similar data for carbon (the only difference being that the Mn concentration is fixed at 1 wt.%.). The explanation is identical to that for the Mn data.

For welds similar to the carbon series, but with the carbon concentration fixed at 0.07 wt.%, the oxygen concentration alone was varied to a range well outside of the training dataset. These results are presented in Fig. 7 along with the ± 1 standard deviation predicted error bars. It is clear that any attempt to extrapolate beyond the dataset on which the model is based gives predictions which are not terribly useful. The fact that the toughness increases with oxygen at low concentrations is strange since the acicular ferrite content (and indeed all the other inputs) are kept constant. An increase in the oxygen content alone should lead to a deterioration in toughness because of the tendency for non–metallic oxide particles to initiate fracture.

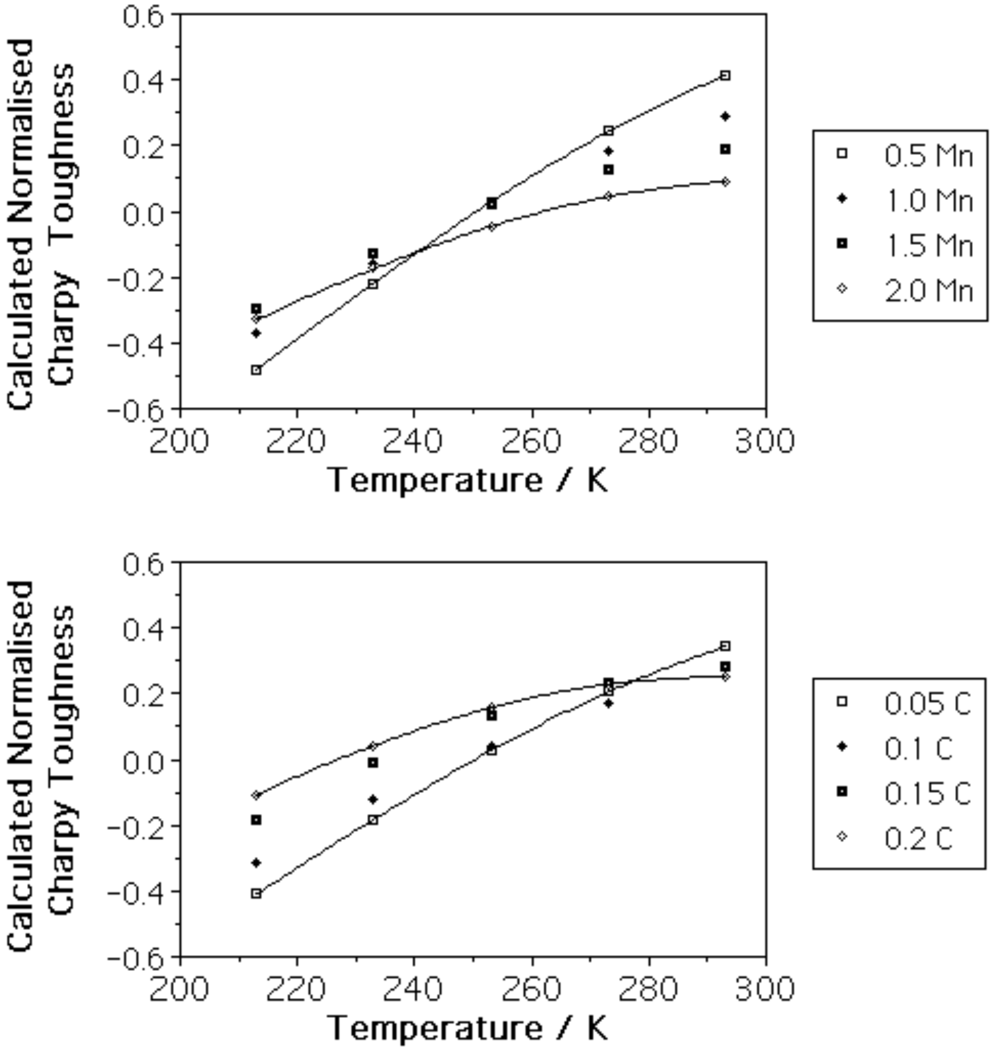

Fig. 6: (a) Variation in the normalised toughness as a function of the manganese concentration. (b) Variation in the normalised toughness as a function of the carbon concentration.

Finally, it is possible using the model to examine effects which cannot easily be produced experimentally. It has frequently been argued that acicular ferrite is a better microstructure than Widmanstätten ferrite, because the former with its less organised arrangement of ferrite plates has a greater capacity to deflect cracks. This was tested for a manual metal arc weld containing 0.07 wt.% carbon but of otherwise identical composition to the carbon series of welds (Fig. 6). The allotriomorphic ferrite fraction was set to zero and all inputs except acicular ferrite and Widmanstätten ferrite were varied in a complementary fashion. The results (Fig. 8) are exciting – they demonstrate that increased acicular ferrite leads to an improvement of cleavage

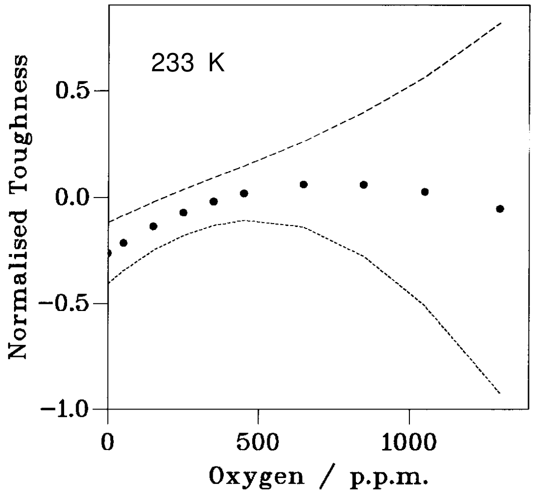

Fig. 7: Variation in the normalised toughness as a function of the oxygen concentration. Oxygen is varied here without changing any of the other inputs. The oxygen concentration in the training data was in the range 234–821 p.p.m.

toughness but not of the upper shelf energy – the latter is not expected to change since the strengths of acicular and Widmanstätten ferrite are virtually identical [24].

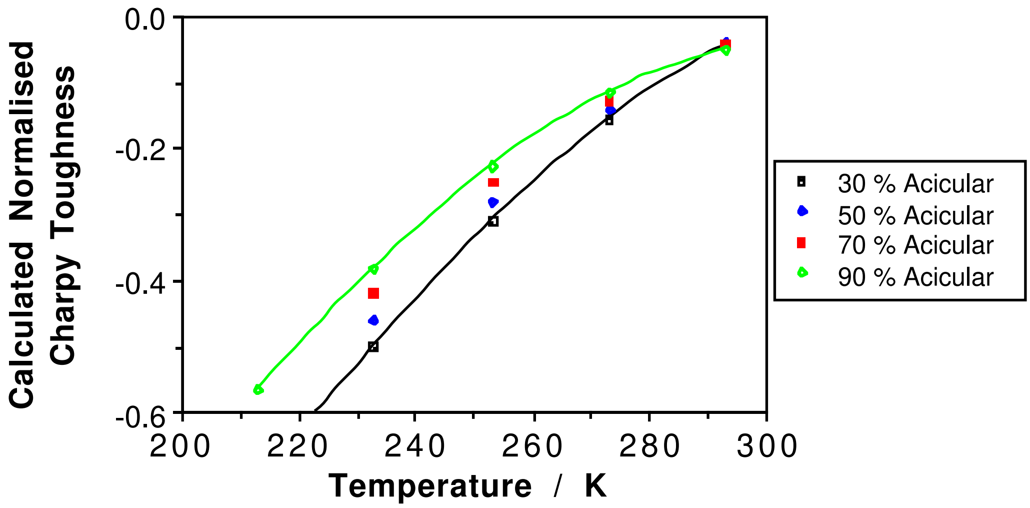

Fig. 8: Variation in the normalised toughness as a function of the acicular ferrite/Widmanstätten ferrite content, everything else being kept constant.

CONCLUSIONS

An artifical neural network has been used to rationalise Charpy impact toughness data on manual metal arc and submerged arc steel weld deposits. The analysis is empirical but after appropriate training, is found to reliably reproduce known metallurgical experience.

The method is useful in that the optimised network summarises knowledge in a quantitative manner and can be retrained as new data become available.

ACKNOWLEDGEMENTS

We are grateful to the Education and Research Committee of Darwin College for fostering an environment in which interdisciplinary learning flourishes.

REFERENCES

1 . J. F. Knott: *Fundamentals of Fracture Mechanics* Butterworths, London, (1973) 8.

2 . O. M. Akselsen and ϕ. Grong: *Materials Science and Engineering A* **A159** (1992) 187–192.

3 . D. E. Rumelhart, G. E. Hinton and R. J. Williams: *Nature (London)* **323** (1986) 533–536.

4 . D. J. C. MacKay: *Neural Computation* **4** (1992) 415–447.

5 . D. J. C. MacKay: *Neural Computation* **4** (1992) 448–472.

6 . D. J. C. MacKay: *Network* (1994) review article, in press.

7 . D. J. C. MacKay: *Maximum Entropy and Bayesian Methods* ed. G. Heidbreder, Santa Barbara, published by Kluwer, Dordrecht, (1994) in press.

8. H. K. D. H. Bhadeshia: *Recent Trends in Welding Science and Technology* eds. S. A. David and J. M. Vitek, ASM International, Materials Park, OH, USA (1989) 189–198.

9 . H. K. D. H. Bhadeshia and L.–E. Svensson: *Mathematical Modelling of Weld Phenomena,* eds. H. Cerjak and K. E. Easterling, Institute of Materials, London (1993) 109–182.

10 . L.–E. Svensson: *Control of Microstructures and Properties in Steel Arc Welds* CRC Press, Ann Arbor, U.S.A. (1994.)

11 . H. K. D. H. Bhadeshia, L.–E. Svensson and B. Gretoft: *Acta Metallurgica* **33** (1985) 1271–1283.

12 . H. K. D. H. Bhadeshia: *Materials Science and Technology* **8** (1992) 123–133.

13 . ESAB AB: *Internal Report RR 82011* (1982.)

14 . ESAB AB: *Internal Report RC 81033* (1981.)

15 . ESAB AB: *Internal Report CML 85014* (1985.)

16 . L.–E. Svensson, B. Gretoft, A. A. B. Sugden and H. K. D. H. Bhadeshia: *Computer Technology in Welding* Welding Institute, Abington, U. K., paper 24 (1988.)

17 . T. W. Lau, M. M. Sadowsky, T. H. North and G. C. Weatherly: *Welding Metallurgy of Structural Steels* ed. J. Y. Koo, Met. Soc. AIME, Warrendale, PA, USA, (1987) 349–366.

18 . R. B. Oldland: *Australian Welding Research* (Dec. 1985) 31–43.

19 . B. Ahlblom, U. Bergstrom, N. E. Hannerz and I. Werlefors: *WI conference on Residuals and Impurities in Steels* Welding Insititute, Abington, Cambridge, U. K., paper 49 (1986.)

20 . ϕ. Grong, A. O. Kluken and B. Bjornbakk: *Joining and Materials* **1** (1988) 164–169.

21 . H. Y. Liou, C. M. Liao and S. C. Wang: *China Steel Technical Report No. 6* (1992) 30–37.

22 . L.–E. Svensson and B. Gretoft: *American Welding Journal* **69** (1990) 454s–461s.

23 . G. M. Evans: *American Welding Journal* **59** (1980) 67s–75s.

24 . A. A. B. Sugden and H. K. D. H. Bhadeshia: *Metallurgical Transactions A* **19A** (1988) 1597–1602.

APPENDIX

Table 3 contains the values for the weights obtained after completing the training of the network. These data can be used in combination with Table 1 and equations 1–3 in order to use the network to make predictions of weld metal toughness.

Description	Abbreviation	weight
Bias to hidden unit 1	$\theta_1^{(1)}$	-0.139995
Bias to hidden unit 2	$\theta_2^{(1)}$	-0.248802
Bias to hidden unit 3	$\theta_3^{(1)}$	0.589258
Bias to hidden unit 4	$\theta_4^{(1)}$	-0.080140
Bias to output unit	$\theta^{(2)}$	-1.40271
Process to hidden unit 1	$w_{1,1}^{(1)}$	-0.953784
Process to hidden unit 2	$w_{2,1}^{(1)}$	0.455700
Process to hidden unit 3	$w_{3,1}^{(1)}$	0.010017
Process to hidden unit 4	$w_{4,1}^{(1)}$	0.355382
Yield strength to hidden unit 1	$w_{1,2}^{(1)}$	0.599265
Yield strength to hidden unit 2	$w_{2,2}^{(1)}$	-0.396398
Yield strength to hidden unit 3	$w_{3,2}^{(1)}$	-0.195261
Yield strength to hidden unit 4	$w_{4,2}^{(1)}$	-0.051569
Carbon to hidden unit 1	$w_{1,3}^{(1)}$	0.003035
Carbon to hidden unit 2	$w_{2,3}^{(1)}$	0.000652
Carbon to hidden unit 3	$w_{3,3}^{(1)}$	0.002913
Carbon to hidden unit 4	$w_{4,3}^{(1)}$	0.004131
Silicon to hidden unit 1	$w_{1,4}^{(1)}$	-0.052339
Silicon to hidden unit 2	$w_{2,4}^{(1)}$	0.069965
Silicon to hidden unit 3	$w_{3,4}^{(1)}$	-0.088386
Silicon to hidden unit 4	$w_{4,4}^{(1)}$	0.039075
Manganese to hidden unit 1	$w_{1,5}^{(1)}$	-0.009951
Manganese to hidden unit 2	$w_{2,5}^{(1)}$	-0.006226
Manganese to hidden unit 3	$w_{3,5}^{(1)}$	-0.010586
Manganese to hidden unit 4	$w_{4,5}^{(1)}$	-0.008486
Phosphorus to hidden unit 1	$w_{1,6}^{(1)}$	-0.108883
Phosphorus to hidden unit 2	$w_{2,6}^{(1)}$	0.070553
Phosphorus to hidden unit 3	$w_{3,6}^{(1)}$	0.029519
Phosphorus to hidden unit 4	$w_{4,6}^{(1)}$	0.047509
Sulphur to hidden unit 1	$w_{1,7}^{(1)}$	-0.004894
Sulphur to hidden unit 2	$w_{2,7}^{(1)}$	-0.008146
Sulphur to hidden unit 3	$w_{3,7}^{(1)}$	-0.006305
Sulphur to hidden unit 4	$w_{4,7}^{(1)}$	-0.009485

Table 3a: The weights describing the trained network

Description	Abbreviation	weight
Aluminium to hidden unit 1	$w^{(1)}_{1,8}$	0.003158
Aluminium to hidden unit 2	$w^{(1)}_{2,8}$	0.004146
Aluminium to hidden unit 3	$w^{(1)}_{3,8}$	0.001416
Aluminium to hidden unit 4	$w^{(1)}_{4,8}$	0.005775
Nitrogen to hidden unit 1	$w^{(1)}_{1,9}$	0.305801
Nitrogen to hidden unit 2	$w^{(1)}_{2,9}$	0.123011
Nitrogen to hidden unit 3	$w^{(1)}_{3,9}$	-0.533206
Nitrogen to hidden unit 4	$w^{(1)}_{4,9}$	0.028576
Oxygen to hidden unit 1	$w^{(1)}_{1,10}$	-0.008650
Oxygen to hidden unit 2	$w^{(1)}_{2,10}$	0.051781
Oxygen to hidden unit 3	$w^{(1)}_{3,10}$	0.333115
Oxygen to hidden unit 4	$w^{(1)}_{4,10}$	-0.204586
Primary Mic. to hidden unit 1	$w^{(1)}_{1,11}$	0.012150
Primary Mic. to hidden unit 2	$w^{(1)}_{2,11}$	-0.020293
Primary Mic. to hidden unit 3	$w^{(1)}_{3,11}$	-0.044580
Primary Mic. to hidden unit 4	$w^{(1)}_{4,11}$	-0.008752
Allotriomorphic to hidden unit 1	$w^{(1)}_{1,12}$	0.025770
Allotriomorphic to hidden unit 2	$w^{(1)}_{2,12}$	-0.018466
Allotriomorphic to hidden unit 3	$w^{(1)}_{3,12}$	0.016131
Allotriomorphic to hidden unit 4	$w^{(1)}_{4,12}$	0.028425
Acicular to hidden unit 1	$w^{(1)}_{1,13}$	-0.074019
Acicular to hidden unit 2	$w^{(1)}_{2,13}$	0.623779
Acicular to hidden unit 3	$w^{(1)}_{3,13}$	0.655171
Acicular to hidden unit 4	$w^{(1)}_{4,13}$	-0.748358
Temperature to hidden unit 1	$w^{(1)}_{1,14}$	-0.077889
Temperature to hidden unit 2	$w^{(1)}_{2,14}$	-0.077859
Temperature to hidden unit 3	$w^{(1)}_{3,14}$	0.138927
Temperature to hidden unit 4	$w^{(1)}_{4,14}$	0.084853
Hidden unit 1 to output unit	$w^{(2)}_{1}$	7.474170
Hidden unit 2 to output unit	$w^{(2)}_{2}$	6.714920
Hidden unit 3 to output unit	$w^{(2)}_{3}$	7.727480
Hidden unit 4 to output unit	$w^{(2)}_{4}$	8.835680

Table 3b: The weights describing the trained network